

1 **Heterologous expression of *Dehalobacter* spp.
2 respiratory reductive dehalogenases in
3 *Escherichia coli***

4 **Running Title:** *Dehalobacter* RDase expression in *E. coli*

5 **Authors:** Katherine J. Picott,^a Robert Flick,^a Elizabeth A. Edwards^a#

6 ^aDepartment of Chemical Engineering and Applied Chemistry, University of Toronto, Toronto,
7 Ontario, Canada

8 #Address correspondence to Elizabeth A. Edwards, elizabeth.edwards@utoronto.ca

9 **ABSTRACT**

10 Reductive dehalogenases (RDases) are a family of redox enzymes that are required for
11 anaerobic organohalide respiration, a microbial process that is useful in bioremediation. Structural
12 and mechanistic studies of these enzymes have been greatly impeded due to challenges in RDase
13 heterologous expression, primarily because of their cobamide-dependence. There have been a few
14 successful attempts at RDase production in unconventional heterologous hosts, but a robust
15 method has yet to be developed. In this work we outline a novel respiratory RDase expression
16 system using *Escherichia coli* as the host. The overexpression of *E. coli*'s cobamide transport
17 system, *btu*, and RDase expression under anaerobic conditions were established to be essential for
18 the expression of active RDases from *Dehalobacter* - an obligate organohalide respiring bacterium.
19 The expression system was validated on six RDase enzymes with amino acid sequence identities
20 ranging from >30-95%. Dehalogenation activity was verified for each RDase by assaying cell-free
21 extracts of small-scale expression cultures on various chlorinated substrates including
22 chloroalkanes, chloroethenes, and hexachlorocyclohexanes. Two RDases, TmrA from

23 *Dehalobacter* sp. UNSWDHB and HchA from *Dehalobacter* sp. HCH1, were purified by nickel
24 affinity chromatography. Incorporation of both the cobamide and iron-sulfur cluster cofactors was
25 verified, and the specific activity of TmrA was found to be consistent with that of the native
26 enzyme. The heterologous expression of respiratory RDases, particularly from obligate
27 organohalide respiring bacteria, has been extremely challenging and unreliable. Here we present a
28 relatively straightforward *E. coli* expression system that has performed well for a variety of
29 *Dehalobacter* spp. RDases.

30 **IMPORTANCE**

31 Understanding microbial reductive dehalogenation is important to refine the global halogen
32 cycle and to improve bioremediation of halogenated contaminants; however, studies of the family
33 of enzymes responsible are limited. Characterization of reductive dehalogenase enzymes has
34 largely eluded researchers due to the lack of a reliable and high-yielding production method. We
35 are presenting an approach to express reductive dehalogenase enzymes from *Dehalobacter*, a key
36 group of organisms used in bioremediation, in *E. coli*. This expression system will propel the study
37 of reductive dehalogenases by facilitating their production and isolation, allowing researchers to
38 pursue more in-depth questions about the activity and structure of these enzymes. This platform
39 will also provide a starting point to improve the expression of reductive dehalogenases from many
40 other organisms.

41 **KEYWORDS:** reductive dehalogenases, heterologous expression, *Dehalobacter*, cobalamin,
42 *Escherichia coli*, enzyme purification, iron-sulfur clusters

43

44

45 INTRODUCTION

46 A wide array of naturally produced halogenated organic compounds, or organohalides, are
47 present in the environment. Organohalides also make up some of the most pervasive and
48 concerning anthropogenic soil, sediment, and groundwater contaminants. Anaerobic
49 organohalide-respiring bacteria (OHRB) can readily degrade a number of these pollutants, such as
50 chlorinated ethenes and ethanes, by using them as terminal electron acceptors in their cellular
51 respiration (1, 2). The respiration process removes halogen atoms from organohalide substrates
52 via reductive dehalogenation, changing the properties of the parent substrate, often detoxifying or
53 transforming them to more degradable substrates for other organisms. OHRB were first described
54 in 1990 (1), and quite rapidly became a staple tool in commercial bioremediation. In particular,
55 obligate OHRB *Dehalococcoides* and *Dehalobacter* are highly abundant in bioremediation
56 cultures targeting chlorinated contaminants (3, 4). Obligate OHRB have very restricted
57 metabolism and can only grow on organohalide substrates while facultative OHRB are flexible
58 and can utilize a variety of electron acceptors (2). All OHRB use reductive dehalogenase enzymes
59 (RDase) discovered in 1995 as part of their electron transport chain to perform these reduction
60 reactions (5). RDases are key targets for studying the mechanism of OHRB respiration and
61 remediation, and on their own RDases offer an intriguing tool for industrial applications.

62 RDases form a large family of oxygen-sensitive enzymes that rely on two iron-sulfur
63 clusters ([4Fe-4S]) and a cobamide, commonly cobalamin or vitamin B₁₂, as cofactors to perform
64 catalysis; RDases are well described in previous reviews (2, 6). There are two broad categories:
65 respiratory RDases from OHRB, and catabolic RDases which are catalytically similar but perform
66 a different cellular function (7, 8). Here we will focus on respiratory RDases as they represent an
67 unusual metabolism and are more relevant to bioremediation. All RDases remove halogen atoms

68 from their substrate through either a hydrogenolysis reaction, where one halogen is substituted
69 with a hydrogen, or a β -elimination reaction, where two halogen atoms across a single bond are
70 removed (this may also occur with a halogen and a hydrogen in a non-energy yielding process).
71 Respiratory RDases also hold a twin arginine translocation (TAT) signal peptide to localize them
72 to the periplasmic membrane, though these are cleaved off in the mature protein. While the RDase
73 family has wide sequence variation, many of the described RDases are from *Dehalococcoides* and
74 *Dehalobacter* and use chloroethenes, chloroethanes, or chlorobenzenes as substrates. Furthermore,
75 obligate OHRB encode dozens of unique *rdhA* genes in their genomes (9); although, majority are
76 not expressed in culture and have unknown functions. Approximately 25 unique RDases have had
77 their substrates experimentally determined (see Table S1 for details), yet there are almost 1000
78 unstudied *rdhA* (RDase homologous genes) sequences in the Reductive Dehalogenase Database
79 (9), and many more in metagenomic surveys such as the ones described in (10, 11). The number
80 of identified *rdhA* sequences continues to climb with more sequencing, yet functional
81 characterization methods lag far behind.

82 The majority of the functionally characterized RDases were purified from their endogenous
83 (or native) producers (Table S1) through extensive methods (5, 12, 21–23, 13–20). Obtaining
84 enough biomass for such purifications is not a trivial undertaking and the purification methods
85 under anaerobic conditions are tedious. Because most OHRB are difficult to grow as they require
86 toxic, poorly soluble, and often volatile halogenated substrates, small scale partial purification
87 using blue native-polyacrylamide gel electrophoresis (BN-PAGE) coupled with activity assays and
88 proteomic analysis has proven very useful for ascribing substrates to specific RDases (24–29). All
89 of the above characterization studies are confined both to lab-cultivable organisms and to
90 actively expressed genes. Table S1/SI Text 1 provides a list of currently known RDases.

91 To address the limitations of purifying RDases from native producers, many research
92 groups have attempted heterologous expression, but the complex cofactor requirements, which are
93 crucial for RDase activity, have hindered efforts. We compiled a list of all expression studies
94 (Table S2/SI Text 1). The first published expression attempt was in 1998, where PceA from
95 *Sulfurospirillum multivorans* was expressed in *Escherichia coli* but no activity detected (30).
96 Subsequent trials in *E. coli* involved denaturation and cofactor reconstitution (31, 32). It was not
97 until 2014 when the first activity from heterologously expressed RDases were from the cobamide
98 producing host *Shimwellia blattae*; however, these enzymes were unable to be purified using a
99 Strep affinity tag (33). Finally, twenty years after their discovery, the first RDase crystal structures
100 were solved: one of PceA from *S. multivorans*; obtained from the native producer with a mutation
101 to incorporate an affinity tag (34), and the catabolic RDase NpRdhA from *Nitratireductor*
102 *pacificus* pht-3B; expressed in the cobalamin producing *Bacillus megaterium* (8). The two crystal
103 structures confirmed that the cobamide cofactor is deeply buried within the enzyme and makes
104 numerous interactions with the peptide sidechains suggesting that it may serve a structural role for
105 proper enzyme folding (8, 34). Most typical heterologous hosts, such as *E. coli*, neither produce
106 cobamides *de novo* nor import the molecule under basal conditions. Since the crystal structures,
107 there have been a couple successful reports of catalytically active RDase expression all using hosts
108 *S. blattae* and *B. megaterium*, both with full cobamide biosynthetic pathways (35, 36). However,
109 less conventional hosts tend to have lower protein yields and have less standardized protocols. The
110 preferable host would be *E. coli* as it grows quickly, is highly engineered to obtain high protein
111 yield, and is amenable to modern molecular biology tools. Thus far, expression attempts using *E.*
112 *coli* have required enzyme denaturation and refolding for cofactor reconstitution to obtain activity
113 (32, 37, 38), but these methods are too unpredictable and unreproducible to be used as a standard

114 expression system. Although developing a generalizable RDase expression system has been a goal
115 in the field for decades, to date, no respiratory RDase has been directly produced from *E. coli* in
116 its active state.

117 Although *E. coli* does not synthesize cobalamin *de novo*, it, like many other organisms,
118 possesses the vitamin B₁₂ salvage pathway (*btu*) to take up cobalamin from the environment (39).
119 This salvage pathway consists of a series of transport proteins: BtuB, a TonB-dependent
120 transporter protein on the outer membrane to import cobalamin into the periplasm; BtuF, a
121 periplasmic protein that will bind free cobalamin; BtuCD, an ABC-transporter that associates with
122 BtuF to import cobalamin into the cytoplasm, a cartoon representation can be found in Figure 1B
123 (40–46). Expression of the *btu* operon is poor under typical growth conditions but can be enhanced
124 with the use of ethanolamine-based media, which forces *E. coli* to use a cobalamin-dependent
125 enzyme, or by induced expression (44, 47). Recently, the Brooker lab developed an expression
126 system for cobalamin-dependent *S*-adenosylmethionine methylases that expressed the entire *btu*
127 operon from *E. coli* under arabinose induction in the vector *pBAD42-BtuCEDFB* (44). The
128 application of this vector greatly enhanced the solubility and activity of several methylases tested
129 (44). Similarly, the catabolic RDase, NpRdhA, had an slight increase in yield and cofactor
130 incorporation when co-expressed with just BtuB (48). Given the success of these expression
131 systems and the hypothesis that the cobamide cofactor supports proper RDase folding, we
132 predicted that implementation of *btu* expression could result in generation of active RDases in *E.*
133 *coli*.

134 In this work, we employ the *pBAD42-BtuCEDFB*, provided by the Booker lab, in several
135 strains of *E. coli* with enhanced iron-sulfur cluster production and maintenance, for the
136 heterologous expression of several respiratory RDases from *Dehalobacter* spp. This expression

137 system is a tremendous steppingstone to advance knowledge about the RDase enzyme family and
138 organohalide respiration, and to facilitate future development in bioremediation.

139 **Materials and Methods**

140 All chemicals and primers were purchased from Sigma-Aldrich (St. Louis, MO, USA)
141 except for antibiotics, terrific broth (TB) media, and Bradford reagent which were purchased from
142 BioRad (Hercules, CA, USA). All gases were supplied from Linde Canada Inc. (Mississauga, ON,
143 Canada). Synthetic genes and the *pET21-hchA* plasmid were synthesized by Twist Bioscience (San
144 Francisco, CA, USA) using codon optimized sequences for TmrA (WP_034377773), CfrA
145 (AFV05253), DcrA (AFV02209), and HchA (IMG Accession: 2823894057). DNA isolations and
146 purifications were done with the QIAprep Spin Miniprep Kit and the QIAquick PCR Purification
147 Kit, and nickel-nitrilotriacetic acid (Ni-NTA) agarose resin was purchased from Qiagen (Hilden,
148 Germany). PCR reagents, restriction enzymes, Gibson Assembly master mix, the 1 kb DNA
149 ladder, and *Escherichia coli* DH5 α were purchased from New England Biolabs (Ipswich, MA,
150 USA). Sanger sequencing was performed by The Centre for Applied Genomics at SickKids
151 Hospital (Toronto, ON, Canada). The *pBAD42-BtuCEDFB* plasmid was generously provided by
152 the Booker Lab (Pennsylvania State University, PA, USA). *E. coli* BL21(DE3) Δ iscR was obtained
153 from Patrick Hallenbeck (49, 50), *E. coli* BL21(DE3) *cat-araC-P_{BAD}-suf*, Δ iscR::kan,
154 Δ himA::Tet^R, abbreviated to *E. coli* ara-Suf Δ iscR, and *E. coli* SuffFeScient were generously
155 provided by the Antony and Kiley Labs (St. Louis University School of Medicine, MO, USA;
156 University of Wisconsin-Madison, WI, USA) (51). The empty *p15TV-L* plasmid is available at
157 Addgene #26093. All buffers used in protein extractions and purifications were purged with N₂
158 gas prior to use.

159

160 **Plasmid Construction and Transformation**

161 Full *tmrA*, *cfrA*, and *dcrA* genes were codon-optimized and ordered as synthetic gene
162 blocks (Supplemental Text 1). Two primer sets were designed for amplification of the genes with
163 extensions to introduce a 15 bp overlap sequence for Gibson Assembly into the linearized *p15TV-*
164 *L* plasmid. One primer pair amplified the TAT signal peptide sequence and introduced a C-terminal
165 x6His tag extension in case the N-terminal tag was cleaved with the endogenous TAT processing
166 machinery, this pair was only designed for TmrA amplification. The second primer pair amplified
167 the gene without the TAT sequence to truncate the cloned gene, the gene began at the previously
168 observed TAT cleavage site (14). Primer sequences and their descriptions are in Table S3/SI Text
169 2. Genes were amplified by PCR using the synthetic genes as the templates. The *p15TV-L* plasmid
170 was linearized by BseRI digestion. The linear plasmid and the amplified gene products were
171 purified with a QIAquick PCR Purification kit. The amplified gene product and the linearized
172 plasmid were ligated by Gibson Assembly, transformed into *E. coli* DH5 α competent cells via
173 chemical transformation, and plated on carbenicillin (100 ng/mL) selection plates.

174 Positive transformants were picked, grown up, and their plasmids were extracted. The
175 plasmids were screened by PCR amplification of the desired gene and Sanger sequencing using
176 universal T7 primers. The sequencing-confirmed plasmids were transformed into both *E. coli*
177 *ΔiscR* and *E. coli ara-Suf ΔiscR* strains with and without *pBAD42-BtuCEDFB*; those with
178 *pBAD42-BtuCEDFB* were selected with carbenicillin and spectinomycin (50 ng/mL) plates. The
179 plasmid *p15TVL-tmrA* was also transformed into *E. coli* BL21(DE3) Lobstr and *E. coli*
180 SufFeScient. The codon-optimized *hchA* gene without the TAT signal sequence, as predicted by
181 SignalP-5.0 (52), was ordered in *pET-21* with a C-terminal x6His tag. The genes for DHB14 and
182 DHB15 had been previously amplified from genomic DNA isolated from the ACT-3 mixed culture

183 and cloned into *p15TV-L* with their TAT signal sequences by the Yakunin and Savchenko Labs
184 (University of Toronto, Toronto, ON, Canada). The plasmids *pET21-hchA*, *p15TVL-DHB14*, and
185 *p15TVL-DHB15* were transformed into *E. coli* Δ *iscR* with *pBAD42-BtuCEDFB*. Descriptions of
186 all expression plasmids are included in Table S4/SI Text S2, and descriptions of the *E. coli* strains
187 used are in Table S5/SI Text S2.

188 **Small-Scale Protein Expression and Lysis**

189 Full schematic of small-scale expression and lysate activity assays is shown in Figure 1.
190 An aliquot (200 μ L) of starter cultures containing the desired expression plasmids were used to
191 inoculate 20 mL of TB media with the appropriate antibiotics in 160 mL serum bottles, or 250 mL
192 Erlenmeyer flasks if full expression was aerobic. In initial tests to establish the expression system,
193 cultures in the serum bottles were grown anaerobically by sealing the bottle and purging the media
194 with N_2 prior to inoculation, these were then treated the same as the aerobic cultures (same
195 induction and incubation times) though the cell density tended to be lower in these samples. After
196 further optimization the finalized expression system is described here. Bottles and flasks were kept
197 aerobic for growth, and the cultures were incubated at 37°C, 180 rpm until the optical density at
198 600 nm (O.D.₆₀₀) reached 0.4-0.6. Cultures were supplemented with a final concentration of 1 μ M
199 hydroxycobalamin and *btu* expression was induced with a final concentration of 0.2% (w/v)
200 arabinose (regardless of whether *pBAD42-BtuCEDFB* was present in the culture strain). Cultures
201 were incubated again at 37°C, 180 rpm until the O.D.₆₀₀ reached 0.8-1. All cultures were put on
202 ice, cultures in serum bottles were stoppered, crimped, and the headspace was purged with N_2 gas
203 for 10 min to remove excess O_2 , cultures in flasks remained aerobic. All cultures were
204 supplemented with final concentrations of either 50 μ M ammonium ferric sulphate used during
205 TmrA expression optimization, or 50 μ M cysteine and 50 μ M ammonium ferric citrate used with

206 all subsequent cultures to align with recommended iron-sulfur sources though no change in activity
207 was observed (53), and RDase expression was induced using 1 mM isopropyl β -D-1-
208 thiogalactopyranoside (IPTG). Cultures were incubated at 15°C, 180 rpm overnight. Expression
209 of TmrA under different conditions tested is in Figure S1/SI Text 3.

210 After incubation, all cultures were handled in a Coy anaerobic glovebox with a supply gas
211 composition of 10% H₂, 10% CO₂, and 80% N₂. Cultures were harvested by centrifugation at 6000
212 xg (Avanti-JE SN:JSE07L45, Beckmann Coulter) and 4°C for 10 min. Supernatants were
213 discarded and the pellets were resuspended in 1 mL of Buffer A (50 mM Tris-HCl (pH 7.5), 150
214 mM NaCl, 5% glycerol, 0.1% Triton X-100) with 1 mM tris(2-carboxyethyl)phosphine (TCEP)
215 and Protease Inhibitor Cocktail (PIC; final concentrations: 1 mM benzamidine, 0.5 mM
216 phenylmethylsulfonyl fluoride) added fresh at time of use. In some cases, Triton X-100 in Buffer
217 A was replaced with either 1% 3-((3-chloroamidopropyl)dimethylammonio)-1-propanesulfonate
218 (CHAPS) or 1% digitonin. The suspended pellet was transferred to a 2 mL o-ringed
219 microcentrifuge tube with 50 mg of glass beads (150-500 μ m). The cells were lysed via bead
220 beating by vortexing the tubes for 2 min and resting on ice for 1 min, repeated 3 times. The lysate
221 was clarified by centrifugation at 20 000 xg (Thermo Scientific microcentrifuge, serial:
222 1931100817155), 4°C for 5 min. The soluble lysate fraction was used for subsequent activity
223 assays. The positive controls using ACT-3, a mixed culture enriched maintained on either
224 chloroform or 1,1,1-trichloroethane as electron donor, were prepared the same way only 0.5 mL
225 of buffer was used for resuspension.

226

227

228 **TmrA and HchA Large-Scale Protein Expression and Purification**

229 An overnight start culture (5 mL) of either *E. coli* *ara-Suf* Δ *iscR* *p15TVL-tmrA* + *pBAD42-*
230 *BtuCEDFB* or *E. coli* Δ *iscR* *pET21-hchA* + *pBAD42-BtuCEDFB* was used to inoculate 1 L of TB
231 medium with appropriate antibiotics in a 2 L glass bottle (Fischer Scientific), that was kept aerobic
232 for growth with a foil cap. The culture was incubated at 37°C, 150 rpm until the O.D.₆₀₀ reached
233 0.4-0.6, 3 μ M hydroxycobalamin was supplemented to the culture and 0.2% (w/v) arabinose was
234 used to induce *btu* expression. This was incubated at 37°C, 150 rpm again until the O.D.₆₀₀ reached
235 0.8-1, after which the culture was put on ice, sealed with a rubber septa and cap, and the headspace
236 was purged with N₂ gas for 1 hr to make anaerobic. The culture was supplemented with 50 μ M
237 cysteine and 50 μ M ammonium ferric citrate, and RDase expression was induced with 1 mM IPTG.
238 The culture was then incubated overnight at 15°C, 150 rpm.

239 The expression culture was handled in a Coy anaerobic glovebox or kept sealed in an
240 airtight vessel for all of the following steps. The culture was harvested by centrifugation at 6000
241 xg, 4°C for 15 min (Avanti-JE SN:JSE07L45, Beckmann Coulter). The supernatant was discarded,
242 and the pellet was resuspended in 5 mL of Binding Buffer (Buffer A, 30 mM imidazole) per 1 g
243 of wet cell weight with 1 mM TCEP and PIC added fresh to the buffer from concentrated stocks.
244 The cells were lysed with the addition of 10x Bug Buster concentrate (Millipore), at the proper
245 dilution, 0.3 mg/mL lysozyme, 1.5 μ g/mL DNase, and 10 mM MgCl₂ (final concentrations). The
246 lysate was incubated at RT shaking at 50 rpm for 20 min. The lysate was clarified by centrifugation
247 at 29 000 xg, 4°C for 20 min (Avanti-JE SN:JSE07L45, Beckmann Coulter).

248 A 1 mL Ni-NTA resin in a glass gravity-flow column (Econo-Column[®], BioRad, USA)
249 was set up inside a Coy anaerobic glovebox with an atmosphere of 100% N₂. Ni-NTA (1-2 mL)

250 resin was purged with N₂ prior to use. The column was washed with 5 column volumes (CVs) of
251 ddH₂O and conditioned with 5 CVs of Binding Buffer. The clarified cell lysate was loaded onto
252 the column, flow through was collected for subsequent analysis. The column was washed with 20
253 CVs of Binding Buffer until no protein was detected in the eluent by Bradford reagent. The RDase
254 was eluted from the column using Elution Buffer (Buffer A, 300 mM imidazole). Collected
255 fractions underwent a buffer exchange into Buffer A (without imidazole) with 1 mM TCEP, to
256 remove the imidazole and the protein was concentrated using a 30 kDa cut-off Millipore filter tube.
257 The concentrated protein was quantified using a Bradford assay and distributed into aliquots for
258 flash freezing and storage in liquid N₂. All steps of the purification were imaged and analysed by
259 SDS-PAGE, the purity of the final enriched enzyme was estimated by band density using Image
260 Lab v6.1 Software (Bio-Rad Laboratories, Inc.); the SDS-PAGE of TmrA and lane density for
261 purity analysis is shown in Figure S2 and protein yield is in Table S6 of SI Text 3.

262 **Dechlorinating Activity Assays**

263 Initial protein activity assays to test Btu expression and effect of oxygen were carried out
264 in 2 mL reaction volumes, all subsequent assays were done at a volume of 500 μ L to conserve
265 materials. All assays were carried out in glass vials with no headspace and sealed with
266 polytetrafluoroethylene (PTFE)-lined caps, these were set up and incubated under anaerobic
267 conditions in a Coy glovebox with a supply gas composition of 10% CO₂, 10% H₂, and 80% N₂.
268 The assay was carried out in a buffer of 50 mM Tris-HCl (pH 7.5), 2 mM Ti(III) citrate, and 2 mM
269 methyl viologen. Enzyme was added in the form of either 50 μ L soluble cell lysate (100 μ L for 2
270 mL reaction volumes) or 0.3-2 μ g purified TmrA/HchA. All substrates, except the
271 hexachlorocyclohexane (HCH) isomers, were supplemented from saturated water stocks to final
272 concentrations of either 0.05 mM (in the case of perchloroethene), 0.5 mM, or 1 mM using

273 Hamilton glass syringes. HCH was added from a 10 mM stock solution in DMSO to a final
274 concentration of 0.3 mM. Lysate assays were kept at RT overnight (18-24 hr), purified enzyme
275 assays were kept at RT for 1 hr and then were stopped by acidification as described below.

276 All assays were stopped by transferring 0.4 mL (1 mL was taken for reactions with 2 mL
277 total volumes) of the reaction volume into acidified water (pH < 2 using HCl) for a total sample
278 volume of 6 mL; this was sealed in a 10 mL vial for headspace analysis by gas chromatography
279 with flame ionization detection (GC-FID). The assays were all run using the same GC-FID
280 separation method on an Agilent 7890A GC instrument equipped with an Agilent GS-Q plot
281 column (30 m length, 0.53 mm diameter). Sample vials were equilibrated to 70°C for 40 min in an
282 Agilent G1888 autosampler, then 3 mL of the sample headspace was injected (injector set to
283 200°C) onto the column by a packed inlet. The flow rate was 11 mL/min of helium as the carrier
284 gas. The oven was held at 35°C for 1.5 min, raised at a rate of 15°C/min up to 100°C, the ramp
285 rate was reduced to 5°C/min until the oven reached 185°C at which point it was held for 10 min.
286 Finally, the oven was ramped up to 200°C at a rate of 20°C/min and held for 10 min. The detector
287 was set to a temperature of 250°C. Data were analyzed using Agilent ChemStation Rev. B.04.02
288 SP1 software, and peak areas were converted to liquid concentration using standard curves
289 (external calibration) for each compound. An example chromatogram is shown in Figure S3/SI
290 Text 3.

291 Three types of negative controls for the enzyme assays were used: enzyme-free controls,
292 deactivated enzyme controls, and free cobalamin (cobalamin only; no enzyme) controls. Enzymes
293 were deactivated by boiling lysate or purified sample for 5-10 min, this was only done for one
294 representative enzyme for each substrate to verify there was no abiotic reaction from the *E. coli*
295 lysates. Reduction using free cobalamin was tested using a final assay concentration of 0.2 μM

296 cobalamin for lysate assays, and at an equimolar concentration to the enzyme when used as a
297 negative control in the purified enzyme assays. ACT-3 mixed culture was used as a positive control
298 where possible, using 50 μ L of soluble cell lysate, similar to the heterologously expressed
299 enzymes. All enzyme lysates were tested with six replicates (two lysates from independently
300 grown expression cultures with three assays each) on their known substrates to confirm activity,
301 and a minimum of duplicates on additional substrates (two lysates from independently grown
302 cultures). Negative controls for α -HCH were only done as single samples due to limited substrate.
303 The purified TmrA/HchA preparations were tested in triplicates. The number of replicates is
304 indicated where the data are presented, all of the individual sample raw data are shown in excel
305 Tables S7-S11.

306 **Cofactor Quantification**

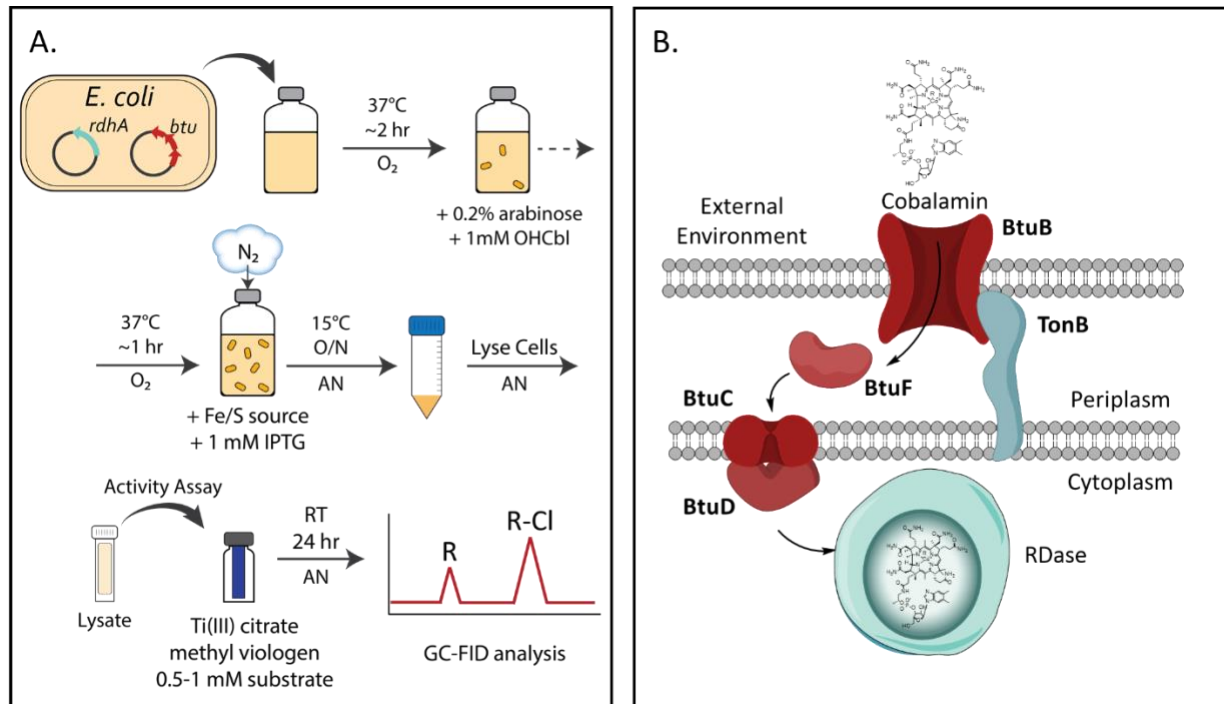
307 Iron content of purified TmrA and HchA was quantified using a ferrozine method as
308 previously described (49, 54, 55). A range of 0.5-20 nmol FeCl₃ was used to create a standard
309 curve. Protein samples were boiled for 5 mins; both the samples and standards were mixed with
310 300 μ L iron-releasing agent (1.4 M HCl, 0.3 M KMnO₄) and heated at 60°C for 30 min. This was
311 brought to RT and then mixed with 150 μ L iron-binding agent (6.5 mM ferrozine, 6.5 mM
312 neocuproine-HCl, 2.5 M ammonium acetate, 1 M ascorbic acid). The absorbance was measured at
313 560 nm and iron content in the protein sample was determined by the standard curve and adjusted
314 with the purity of TmrA/HchA to get an occupancy ratio that was not skewed by the impurities.

315 Cobalamin was quantified using two separate methods, in both cases cyanocobalamin at a
316 concentration range of 0.1-10 μ M (final concentration) was used for a standard curve. The first
317 method was used as previously described with some modifications (35, 44, 56). The standard
318 samples and protein samples (50 μ L) were mixed with 15 mM KCN to a volume of 750 μ L and

319 were heated at 80°C for 10 min. The samples were clarified by centrifugation and their absorbance
320 was measured at 367 nm and at 650 nm to normalize to the baseline. The second method was
321 previously described (57, 58); briefly, samples were mixed with 10 mM KCN in 80% (v/v)
322 methanol and acidified using 3% (v/v) acetic acid. Samples were then heated at 80°C for 1 hr with
323 slow shaking. Samples were clarified by centrifugation, the supernatant was transferred and dried,
324 and the extract was resuspended in ddH₂O such that the concentration was unaltered. These
325 samples were analysed using ultra-high performance liquid chromatography-mass spectrometry
326 (UHPLC-MS). For both methods the cobalamin occupancy was adjusted for the purity of the
327 enzymes.

328 The samples analyzed by UHPLC-MS were separated on a Thermo Scientific Ultimate
329 3000 UHPLC instrument equipped with a Thermo Scientific Hypersil Gold C18 column (50 × 2.1
330 mm, 1.9 µm particle size) and a guard column held at 30°C. The sample (10 µL) was injected by
331 an autosampler held at 5°C. Eluent A was 5 mM ammonium acetate in water, eluent B was 5 mM
332 ammonium acetate in methanol, the flow rate was set to 300 µL/min. The separation method used
333 started with a mix of 2% eluent B for 0.46 min, then held a linear gradient to 15% B from 0.46-
334 0.81 min; a linear gradient to 50% B from 0.81-3.32 min; a linear gradient to 95% B from 3.32-
335 5.56 min; 95% B was held until 7.5 min; finally, the composition was reduced to 2% B with a
336 linear gradient from 7.5-8 min, and held at 2% B from 8-12 min. The eluent was introduced to a
337 Thermo Scientific Q Exactive mass spectrometer with a heated electrospray ionization (HESI-II)
338 probe at a spray voltage of 3.5 kV, and capillary temperature of 320°C. Data collection was done
339 in positive ion modes with a scan range of 1000-2000 m/z, mass resolution of 70 000, an automatic
340 gain control target of 3×10⁶, and a maximum injection time of 200 ms. Data were processed using

341 Thermo Xcalibur Qual Browser v3.1 software, cyanocobalamin was detected at an $[M + H]^+$ of
342 1355.5747 (ppm error = 5), the peak area was used for quantification.



343
344 Figure 1. (A) Schematic of the RDase expression system and small-scale expression tests to
345 determine production of the active RDases. (B) Cartoon of the Btu pathway used for cobalamin
346 incorporation in RDase expression, figure adapted from (44). O₂ = aerobic conditions, AN =
347 anaerobic conditions, O/N = overnight, GC-FID = gas chromatography with flame ionization
348 detection.

349 RESULTS & DISCUSSION

350 Developing the expression system in *E. coli*.

351 The expression system was developed using TmrA, a chloroalkane-reducing RDase from
352 *Dehalobacter* sp. UNSWDHB. It was chosen because it was previously expressed in its active
353 form in *B. megaterium* (35). TmrA was cloned without its TAT signal peptide into the *p15TV-L*

354 expression vector. This construct expressed TmrA with an N-terminal x6His tag under IPTG
355 control. The expression vector was introduced into *E. coli* $\Delta iscR$, a strain engineered for enhanced
356 [4Fe-4S] production by deleting the *isc* (iron-sulfur cluster) operon repressor (49, 50). Small-scale
357 expression cultures were used to test TmrA production in a variety of conditions; a schematic of
358 the final protocol is shown in Figure 1. To establish necessary conditions for successful expression,
359 TmrA was initially tested with and without *pBAD42-BtuCEDFB* for *btu* operon co-expression
360 (44), and in the presence and absence of oxygen during induction. While TmrA expression was
361 evident in all conditions (Figure S1/SI Text 3), its solubility in each case was difficult to distinguish
362 as very little enzyme was visible and overlapped with the host's proteins. For this reason, an
363 activity assay, specifically the level of chloroform reduction observed from soluble lysate fraction,
364 was used to indicate the relative production of active TmrA under each set of conditions. All assays
365 were performed under anaerobic conditions using titanium(III) citrate as the reductant, and methyl
366 viologen as the electron donor. The assay results were measured by end-point detection after 18-
367 24 hr using GC-FID to quantify the substrate and product(s). We found that the co-expression of
368 the *btu* operon paired with TmrA induction under anaerobic conditions was essential to produce
369 active TmrA in *E. coli* (Figure 2A). Under these two conditions 76 ± 4 nmol of dichloromethane
370 (DCM) was produced (significantly higher than the limit of detection of 5 nmol for DCM on this
371 instrument), whereas with no Btu co-expression or in the presence of oxygen no DCM was
372 detected.

373 A variety of additional conditions were tested to see if the observed activity could be
374 enhanced, these included: varying lysis buffer detergent, inclusion of the TAT signal peptide, and
375 testing different *E. coli* strains. The detergents tested were 0.1% Triton X-100, 1% CHAPS, and
376 1% digitonin; there was only a minor difference in DCM production between these detergents (82

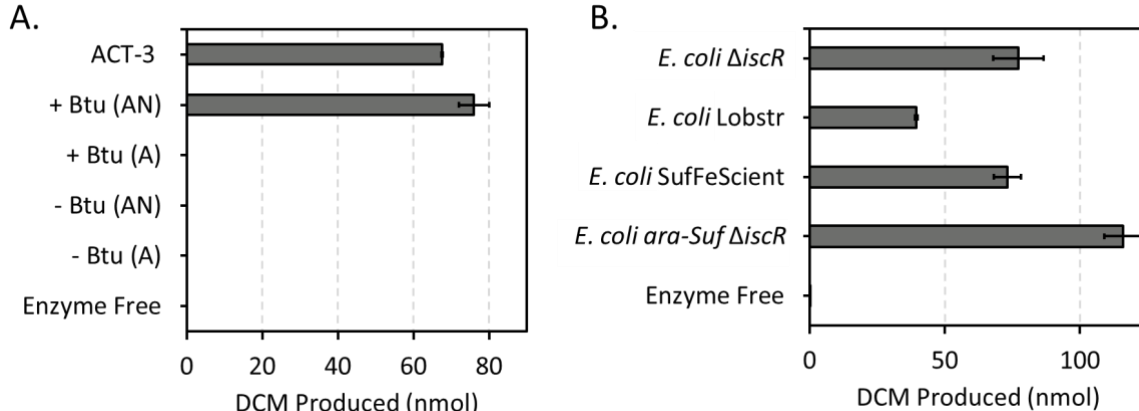
377 \pm 1, Triton X-100; 76 \pm 2, digitonin; 67.9 \pm 0.3, CHAPS), so all subsequent experiments were
378 continued with Triton X-100. However, this flexibility may not be true for all RDases as some
379 *Dehalococcoides* RDases were shown to be inhibited by certain detergents (59). The inclusion of
380 the TAT sequence when expressing TmrA also did not have a notable effect on the enzyme
381 activity; although, it could interfere with downstream applications, so we chose to use the truncated
382 TmrA. Finally, we tested three different strains of *E. coli* that have enhanced [4Fe-4S] production:
383 *E. coli* Δ iscR (49, 50), *E. coli* SufFeScient (51), and *E. coli* ara-Suf Δ iscR, as well as one typical
384 expression strain, *E. coli* BL21(DE3) Lobstr. Lysates from *E. coli* Δ iscR and SufFeScient had
385 similar levels of chloroform reduction, whereas there was a 30% increase in activity observed from
386 TmrA expressed in *E. coli* ara-Suf Δ iscR (Figure 2B). All the [4Fe-4S] strains displayed at least
387 double the activity as the typical strain *E. coli* Lobstr. *E. coli* ara-Suf Δ iscR was subsequently used
388 as the primary expression strain, unless the RDase of interested displayed poor expression in this
389 strain, in which case *E. coli* Δ iscR was used.

390

391

392

393



394

395 Figure 2. Reduction of chloroform to dichloromethane (DCM) by *E. coli* cell-free extracts
396 expressing TmrA over a period of 24 hr. (A) Comparison of TmrA expressed in *E. coli* ΔiscR with
397 (+ Btu) and without (- Btu) *pBAD42-BtuCEDFB* plasmid expression, and with induction under
398 anaerobic (AN) or aerobic (A) conditions. (B) Comparison of TmrA expressed in different *E. coli*
399 strains with *pBAD42-BtuCEDFB* co-expression and under anaerobic conditions. ACT-3 mixed
400 culture cell-free extract was used as a positive control and an enzyme free negative control was
401 used. Error bars are standard deviation between replicates (n = 6, except for ACT-3, enzyme free,
402 and aerobic samples where n = 3).

403

404 The implementation of the *pBAD42-BtuCEDFB* plasmid to increase the uptake of
405 cobalamin was key and essential to successful expression. It is now well known that a cobamide
406 co-factor is critical to protein folding and activity in RDases. The requirement of a cobamide
407 during protein expression, in previous studies and this work, and its buried position within the
408 known crystal structures suggests that the cobamide is needed for the enzyme to fold into its
409 catalytically active form. Induction under anaerobic conditions was also necessary, most likely to
410 prevent oxidative damage to the [4Fe-4S] clusters, but perhaps the addition of a strong reductant

411 into the medium could allow for aerobic induction. The use of *E. coli* strains with increased [4Fe-
412 4S] cluster production or stability also improved the level of activity seen in the lysates compared
413 to conventional strains (Figure 2B). These clusters are essential for electron transport within the
414 enzyme. The specific strain of *E. coli* used for [4Fe-4S] production may depend on the desired
415 RDase as the expression levels of some enzymes varied depending on the strain. Overall, this
416 expression system successfully reached the goal of producing active respiratory RDases in *E. coli*.
417 Furthermore, this expression system was successful on an RDase from the obligate OHRB
418 *Dehalobacter* and may be particularly useful for studying the organohalide respiration process.

419 The only other account of *E. coli* being used for the production of a functional RDase,
420 without cofactor reconstitution, was the expression of NpRdhA (48). Similarly, the authors
421 improved cobalamin transport to support expression and cofactor incorporation (48). However,
422 NpRdhA, being a non-respiratory metabolic (i.e., not membrane associated) RDase which acts on
423 relatively soluble halogenated phenols and hydroxybenzoic acids, is itself more soluble and more
424 oxygen tolerant than respiratory RDases. NpRdhA was expressed in a conventional *E. coli* strain
425 both with and without the co-expression of BtuB from the *btu* operon (48). The addition of the
426 BtuB co-expression increased the cobalamin occupancy by 9% and doubled the enzyme yield (48),
427 but was not a determining factor in the production of active protein, contrary to what we observe
428 from the respiratory RDases. NpRdhA is not a suitable comparator for the systems presented here.

429 **Comparing heterologous RDase substrate specificity**

430 We applied the optimized expression system to a series of other enzymes to validate its
431 reproducibility. CfrA and DcrA, chloroethane reductases from *Dehalobacter* sp. CF and DCA,
432 respectively, in the ACT-3 mixed culture, were chosen to be tested as they have >95% amino acid
433 sequence identity to TmrA but have displayed differing substrate preferences when isolated and

434 tested from their native producers (14, 27). CfrA was experimentally shown to reduce chloroform
435 and 1,1,1-trichloroethane (1,1,1-TCA) but not 1,1-DCA; DcrA accepts 1,1-dichloroethane (1,1-
436 DCA) as a substrate, but not 1,1,1-TCA or CF; and TmrA accepts all three substrates (14, 27). As
437 well, 1,1,2-trichloroethane (1,1,2-TCA) is a substrate for all three enzymes, although the products
438 of reaction vary as 1,1,2-TCA can undergo both dihaloelimination or hydrogenolysis (14, 60).
439 DcrA has not been explicitly assayed against 1,1,2-TCA, but the organism that it comes from can
440 use 1,1,2-TCA as an electron acceptor so it has assumed activity on this substrate (60). The known
441 distinction between these enzymes' substrate ranges made them good subjects to confirm that the
442 expressed enzymes exhibit the same specificity. Both CfrA and DcrA were successfully expressed
443 in small-scale cultures and the resulting cell lysates displayed activity on their expected substrates.

444 TmrA, CfrA, and DcrA were all assayed against several chloroalkanes: chloroform,
445 1,1,1-TCA, 1,1,2-TCA, and 1,1-DCA. The amount (nmol) of each dechlorinated product produced
446 in the assays are given in Table 1, some substrates yielded multiple products depending on the
447 reaction pathway. Heat deactivated controls were used for each substrate, none of which showed
448 notable reduction of the substrate except 1,1,1-TCA to 1,1-DCE though this transformation was
449 also seen in the enzyme free control (Table S8). While the specific activity of each enzyme cannot
450 be compared from the lysate assays as the amount of RDase is unknown, their substrate preferences
451 and products can be compared. TmrA and CfrA both reduced chloroform, 1,1,1-TCA, and 1,1,2-
452 TCA via hydrogenolysis; although, TmrA transformed a considerable amount of 1,1,2-TCA into
453 the β -elimination product, vinyl chloride (VC), while CfrA only produced a minute amount of VC.
454 TmrA was also able to reduce 1,1-DCA to chloroethane (CA) while CfrA had negligible activity
455 on this substrate consistent with previous studies (27). In contrast, DcrA reduced 1,1-DCA, but
456 was not active on CF and barely on 1,1,1-TCA (Table 1), also consistent with previous studies

457 (27). The one surprising result was the high production of 1,1-DCE from 1,1,1-TCA as this is only
458 a minor by-product in the cultures and is mainly thought of as an abiotic reaction (61). Since 1,1-
459 DCE is also seen in the negative controls we anticipate it to be an abiotic reaction accelerated by
460 a component of the buffer. The observed substrate selectivity, particularly those of CfrA and DcrA,
461 act as validation that the heterologously expressed enzymes behave similarly to those partially
462 purified and characterized from the native organisms.

463 Table 1. Reduction of chlorinate substrates over 24 hr by the cell extracts of *E. coli* expressing
464 TmrA, CfrA, and DcrA. All assays were done with approximately 4-10 µg of total protein. Error
465 is the standard deviation between replicates, number of replicates are indicated for each sample.

	Enzyme-Free	TmrA	CfrA	DcrA
Known Substrates		CF; 1,1,1-TCA; 1,1,2-TCA; 1,1-DCA	CF; 1,1,1-TCA; 1,1,2-TCA	1,1-DCA; 1,1,2-TCA
Substrate	Product(s)	Amount Produced (nmol)		
CF	DCM	n.d. ^a	101± 7 ^b	90 ± 10 ^b
1,1,1-TCA	1,1-DCA	0.09 ± 0.06 ^a	7 ± 3 ^b	13 ± 1 ^b
	1,1-DCE*	1.3 ± 0.3 ^a	12.4 ± 0.8 ^b	11.7 ± 0.2 ^b
1,1,2-TCA	1,2-DCA	n.d. ^a	38 ± 6 ^c	35 ± 5 ^c
	VC*	n.d. ^a	11 ± 2 ^c	0.4 ± 0.2 ^c
1,1-DCA	CA	n.d. ^a	9 ± 5 ^c	0.07 ± 0.05 ^c
	VC*	n.d. ^a	n.d. ^c	0.04 ± 0.03 ^b

466 CF = chloroform, DCM = dichloromethane, TCA = trichloroethane, DCA = dichloroethane, VC =
467 vinyl chloride, CA = chloroethane, n.d. = not detected

468 * β -elimination pathway, ^an = 2, ^bn = 6, ^cn = 4

469

470 The successful expression of CfrA and DcrA was expected after optimizing the system on
471 TmrA since the enzyme sequences are almost identical to each other and are thus likely to behave
472 similarly. While these three enzymes have been previously studied, it was still intriguing to remove
473 any other biological factors from the native organisms and confirm their unique substrate
474 preferences in a heterologous system. In agreement with the literature, CfrA was much more
475 efficient at reducing trichloroalkanes, whereas DcrA can almost exclusively reduce 1,1-DCA (27).
476 TmrA displays activity against all the chloroalkanes assayed, and reduced 1,1,2-TCA to both 1,2-
477 DCA and VC. The observed activity differences by each of these enzymes confirms that it is their
478 amino acid sequence that affects their activity and not external factors such as the type of
479 cobamide, protein-protein interactions, or other cellular components.

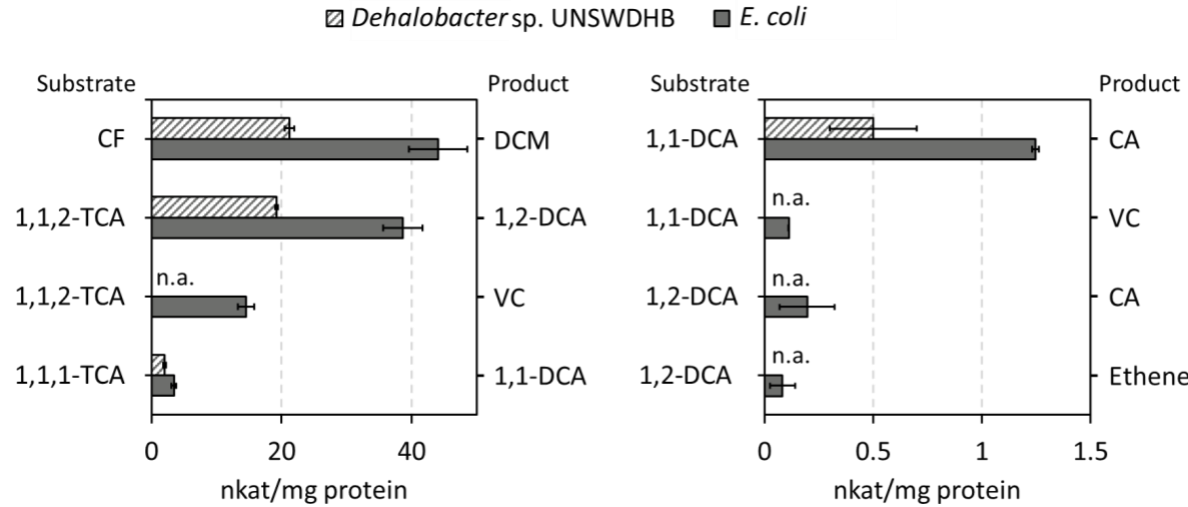
480 **TmrA purification and specific activity**

481 TmrA was elected for large scale purification trials because TmrA has published activity
482 and expression data to compare against. TmrA was semi-purified from a 1 L expression culture
483 using nickel affinity chromatography. An SDS-PAGE of the TmrA purification is shown in Figure
484 S2A/SI Text 3. The concentrated protein sample was a yellow-brown colour indicating the
485 presence of [4Fe-4S] clusters. TmrA was purified to an approximate purity of 50%, 2.2 ± 0.2 mg
486 of protein was obtained from about 7.5 g wet cell mass. For details about the purification and purity
487 estimation see Figure S2B and Table S6 of SI Text 3. To further assess the quality of the
488 purification, the cofactors were extracted and quantified to measure their occupancy ratio. RDases
489 are expected to have eight iron atoms from two [4Fe-4S] clusters. After adjusting for purity (i.e.,
490 assume the cofactors were only coming from TmrA), TmrA was found to have 6.2 ± 0.6 mol iron
491 per mol enzyme. The cobalamin occupancy was measured by two methods; the first was extracted
492 into water and measured by absorbance at 367 nm, characteristic of dicyanocobalamin. Using this

493 method and correcting for purity, TmrA was estimated to have cobalamin occupancies of $62 \pm$
494 13% for TmrA. However, using the second method which involved extraction into acidified
495 methanol and quantification by UHPLC-MS and correcting for purity, the enzymes occupancies
496 were measured to be $24 \pm 2\%$. Finally, we found that TmrA was able to withstand freeze-thaw
497 cycles without loss of activity and was able to retain all activity after being exposed to O₂ for 3 hr
498 with 1 mM TCEP in the buffer (longer periods have not been tested; data not shown).

499 The specific activity of TmrA was determined for several substrates; specific activity was
500 reported in nkat (nmol product/s) per mg protein. TmrA activity was measured for all of its known
501 substrates that showed activity in the lysate assays. Assays with the purified enzyme also identified
502 other transformations that were not observed in lysate, such as 1,2-DCA to CA and VC, as well as
503 1,1-DCA to VC. TmrA had the highest specific activity towards chloroform and 1,1,2-TCA into
504 both 1,2-DCA and VC, whereas it had low specific activity towards 1,1,1-TCA and the less
505 chlorinated substrates 1,1-DCA and 1,2-DCA (Figure 3). When concentrated, TmrA was observed
506 to reduce the dichloroethanes and perform both hydrogenolysis and β -elimination reactions on all
507 chloroethane substrates. The reduction of 1,1,1-TCA to 1,1-DCE is not shown as there were similar
508 concentrations in the enzyme-free negative controls so the biotic activity could not be
509 distinguished (Table S11). There was also production of 1,1-DCE in the lysate samples, though
510 the production from the enzymes was 10-fold higher than the enzyme-free control. In the purified
511 protein case, the production levels were equivalent to the negative control which highly suggests
512 it is not a biotic reaction.

513



514
515 Figure 3. Specific activity of TmrA for substrate-product transformations, where nkat is defined
516 as the rate of product formation in nmol/s. Data for TmrA purified from the endogenous host
517 *Dehalobacter* sp. UNSWDHB (striped bars) (14), and TmrA heterologously expressed and
518 purified from *E. coli* (solid bars) are shown. Substrates are indicated on the left axis label and
519 product is indicated on the right axis label. Error bars are from reported standard deviation for the
520 literature values, and the standard deviation of purified enzyme assays (n = 3). n.a. = not available.

521
522 Not only did the substrate profiles match the literature, the purified TmrA had a specific
523 activity that corresponded well to the native enzyme purified from *Dehalobacter* sp. UNSWDHB.
524 The native enzyme was found to be most active on CF and 1,1,2-TCA, and its specific activity
525 towards its substrates was within the same magnitude of the heterologously expressed TmrA
526 (Figure 3). This consistency between the enzymes confirms that the heterologous system is
527 representative of the native enzymes.

528 The use of *E. coli* as the heterologous host has several advantages over the hosts previously
529 used for respiratory RDases, namely *S. blattae* and *B. megaterium*. One advantage is higher protein

530 yields in *E. coli*. From 1 L of culture, we were able to obtain approximately 2 mg of TmrA whereas
531 to get 0.9 mg of TmrA at a similar purity, 15 L of *B. megaterium* was required (35). Furthermore,
532 the RDase expression vectors can be commercially produced in typical *pET* vectors while those
533 for *B. megaterium* and *S. blattae* generally have to be manually cloned (33, 35, 36). The cofactor
534 occupancy of the RDases from this *E. coli* expression system are also comparable to other
535 heterologous hosts. The molar ratio of iron to enzyme was reported to be 7.26 ± 0.48 mol iron/mol
536 TmrA produced in *B. megaterium* and we measured 6.2 ± 0.6 mol iron/mol TmrA from our system
537 (35). TmrA from *B. megaterium* was calculated to have $52 \pm 3\%$ cobalamin occupancy (35), using
538 a similar absorbance based method we measured an occupancy of $62 \pm 13\%$. Although, the
539 variation in cobalamin occupancy measured between the two methods used in this study suggests
540 that the true occupancy is within 20-60%. Our system seems to perform similarly to those using
541 alternative heterologous hosts, is reproducible, and facilitates high-throughput protein production.

542 **Expression and purification of a lindane reductase**

543 HchA, identified from *Dehalobacter* sp. HCH1 as a lindane or γ -hexachlorocyclohexane
544 (γ -HCH) reductase (62), was chosen to test the generalizability of the expression system because
545 it has low amino acid sequence identity (32.8%) to TmrA. This enzyme was recently identified
546 using BN-PAGE in enrichment cultures that dechlorinate HCH via three sequential dechlorination
547 steps to form monochlorobenzene (MCB) and benzene (62, 63). HchA was successfully expressed
548 and was assayed on several of the chlorinated solvents as well as on two isomers of HCH (γ -HCH
549 and α -HCH).

550 HchA produced primarily monochlorobenzene (MCB) from its known substrate γ -HCH
551 (Table 2). Interestingly, it transformed more of the α -HCH isomer and to a higher proportion of
552 benzene. However, there was significant reduction of both isomers by the HchA heat-killed

553 controls and by free cobalamin (Table 2), so the biotic activity needed to be further confirmed (see
554 below). HchA was also able to take 1,1,2-TCA as a substrate and transform it to VC to a greater
555 extent than the cobalamin negative control. Some highly chlorinated substrates, such as γ -HCH
556 and 1,1,2-TCA, are more susceptible to abiotic reduction, whereas others including chloroform are
557 much more resistant to reduction. HchA readily dechlorinated these permissive substrates and
558 primarily seems to catalyze dihaloelimination reactions.

559 Table 2. Reduction of chlorinate substrates over 24 hr by the cell extracts of *E. coli* expressing
560 HchA and the relevant negative controls. All assays were done with approximately 4-10 μ g of total
561 protein, or 100 nmol of hydroxycobalamin. Error is standard deviation of replicates; number of
562 replicates is indicated for each sample.

Substrate	Product(s)	HchA	Heat Killed HchA	Cobalamin	Catalyst Free
		Amount Produced (nmol)			
CF	DCM	n.d. ^a	n.t.	n.t.	n.d. ^a
1,1,2-TCA	1,2-DCA	n.d. ^a	n.t.	n.d.	n.d. ^a
	VC*	18 \pm 6 ^a	n.t.	9.5	n.d. ^a
1,1-DCA	CA	n.d. ^a	n.t.	n.t.	n.d. ^a
γ -HCH	MCB	7 \pm 1 ^b	7.3 \pm 0.7 ^c	9 \pm 2 ^a	0.4 \pm 0.1 ^c
	Benzene	0.07 \pm 0.07 ^b	0.12 \pm 0.07 ^c	0.21 \pm 0.04 ^a	0.07 \pm 0.05 ^c
α -HCH	MCB	18 \pm 1 ^a	n.t.	5.1	0.58
	Benzene	0.6 \pm 0.1 ^a	n.t.	0.15	n.d.

563 CF = chloroform, DCM = dichloromethane, TCA = trichloroethane, DCA = dichloroethane, VC =
564 vinyl chloride, CA = chloroethane, MCB =monochlorobenzene, n.d. = not detected, n.t. = not
565 tested

566 * Dihaloelimination pathway, ^an = 2, ^bn = 6, ^cn = 3.

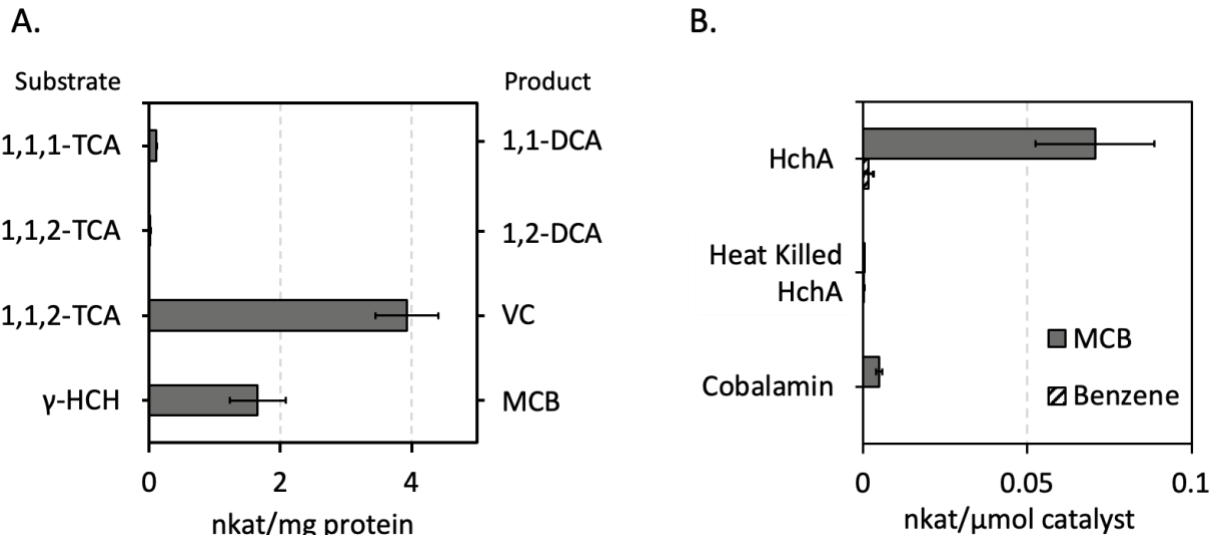
567

568 To probe relative importance of biotic and abiotic reduction of γ -HCH, HchA was scaled
569 up and purified using the same methods as TmrA. HchA was enriched to 39% purity and 2.7 ± 0.4
570 mg of protein was obtained from about 7 g wet cell mass. For details about the purification see
571 Table S6/SI Text 3. The cofactors were also quantified to estimate their occupancy. HchA was
572 found to have 6.4 ± 0.8 mol iron per mol enzyme, a cobalamin occupancy of $76 \pm 14\%$ using the
573 UV-Vis method, and a cobalamin occupancy of $22.1 \pm 0.7\%$ using the LC-MS method. These
574 numbers are consistent with what was observed for TmrA. HchA was also found to be tolerant of
575 freeze-thaw cycles and retained all activity after 30 min of O₂ exposure (with 1 mM TCEP), but
576 only held $60 \pm 35\%$ of its activity after 1 hr of exposure (data not shown).

577 HchA specific activity was measured on γ -HCH, 1,1,2-TCA, and 1,1,1-TCA. HchA had
578 the highest level of activity transforming 1,1,2-TCA to VC, whereas it showed minor
579 transformation of 1,1,2-TCA to 1,2-DCA (0.02 ± 0.01 nkat/mg) and 1,1,1-TCA to 1,1-DCA (0.11
580 ± 0.01 nkat/mg; Figure 4A). The activity on its primary substrate γ -HCH to MCB was 1.7 ± 0.4
581 nkat/mg, the transformation to benzene was not shown as it was also produced in the negative
582 controls. Since the reduction of γ -HCH can also occur abiotically by free cobalamin, the rate of
583 reduction was compared when normalized by mol of catalyst (i.e., HchA and cobalamin). HchA
584 was approximately fourteen times faster than the abiotic reaction (Figure 4B). Further, the killed
585 control of HchA no longer had significant activity indicating that the activity seen in the lysates
586 was most likely due to free cobalamin and longer incubation periods. These results suggests that
587 though γ -HCH is reduced by free cobalamin, the enzyme is clearly more effective.

588

589



590
591 Figure 4. (A) Specific activity of HchA for substrate-product transformations. (B) The rate of
592 monochlorobenzene (MCB) and benzene production from purified HchA, heat killed HchA, and
593 free cobalamin (same molarity of catalysts were used). The nkat is defined as the rate of product
594 formation in nmol/s, this rate is normalized to mols of catalyst. Error bars are the standard deviation
595 between assays (n = 3).

596

597 Further, HchA displayed activity that was not tested previously, most likely due to the limited
598 enzyme available from BN-PAGE separation. HchA was only ever documented to reduce γ -HCH
599 though it seems to be more effective at transforming the alpha isomer and the permissive substrate,
600 1,1,2-TCA. These reactions seen by HchA in the lysates are all expected to be dihaloelimination
601 reactions, but when HchA was concentrated after enrichment it was also observed to have slight
602 hydrogenolysis activity against the 1,1,1-TCA. TmrA was tested against γ -HCH as well but did
603 not catalyze any meaningful transformations (data not shown), suggesting that HchA has some
604 specialization for HCH. HchA poses an interesting comparison to other RDases that predominantly

605 undergo hydrogenolysis reactions to understand how the enzymes distinguish between reaction
606 pathways.

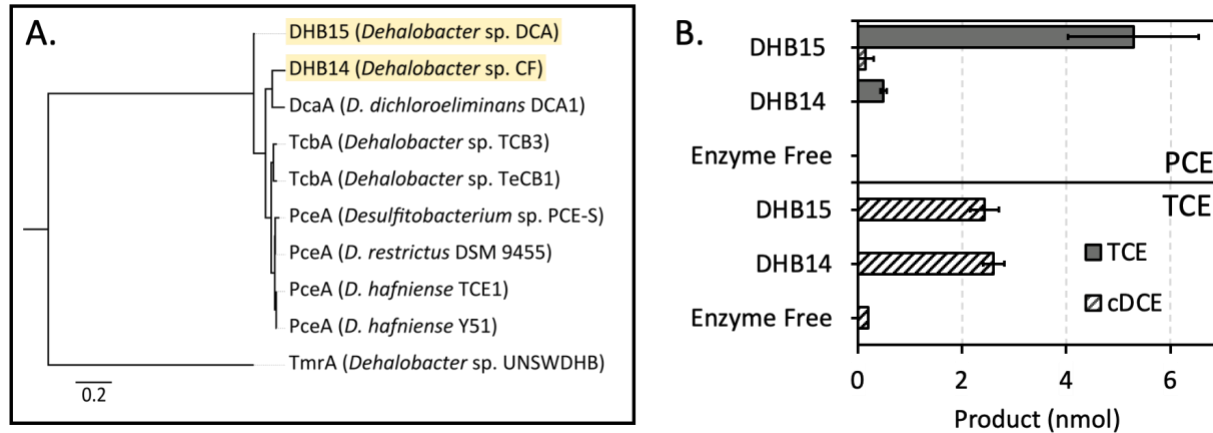
607 **Expression of putative *rdhA* genes**

608 To further test the application of the expression system, we expressed two putative RdhAs,
609 DHB14 and DHB15, that had been previously cloned from the genomic DNA of *Dehalobacter* sp.
610 strains CF and DCA, respectively. These enzymes cluster to a group of *Dehalobacter* and
611 *Desulfitobacterium* RDases including several PceA and TcbA enzymes (Figure 5A), which accept
612 unsaturated and aromatic substrates (29, 31, 64). Based on the similarities to known chloroethene
613 reductases, DHB14 and DHB15 were expressed, the cell lysates were assayed against
614 perchloroethene (PCE) and trichloroethene (TCE), and the presence of dechlorinated products was
615 analyzed (Figure 5B). DHB15 reduced PCE to TCE and a small amount of *cis*-dichloroethene
616 (cDCE), DHB14 only reduced a minor amount of PCE to TCE. Both enzymes reduced a modest
617 amount of TCE to cDCE. The enzymes were also tested for activity on 1,2-dichloroethane (1,2-
618 DCA); however, no product was detected after 24 hr of incubation. The activity of these two
619 enzymes demonstrate that this expression system has potential to functionally characterize the
620 numerous *rdhA* genes encoded in *Dehalobacter* spp. genomes.

621

622

623



625 Figure 5. (A) Maximum-likelihood (ML) tree of DHB14 and DHB15 RdhA amino acid sequences
626 to show relation to the closest characterized RDases in comparison to TmrA. (B) Reduction of
627 either PCE (top) or TCE (bottom) by DHB14 and DHB15 in *E. coli* cell-free extract, assay was
628 done over 24 hr. Error bars are the standard deviation between replicates (n = 4), except negative
629 controls (n = 2). An amino acid alignment was built using the Geneious v8.1.9 MUSCLE plugin,
630 and the ML tree was constructed using RAxML v8.2.12 Gamma GTR protein method with 100
631 bootstraps, the highest scoring tree was selected. Scale indicates average number of substitutions
632 per amino acid site.

633

634 ***Dehalococcoides* RDase expression attempts**

635 The heterologous expression of several RDases from *Dehalococcoides* spp. was attempted
636 using this expression system. Three characterized chloroethene reductases were cloned and
637 expressed: VcrA from *D. mccartyi* VC, BvcA from *D. mccartyi* BAV1, and TceA from *D. mccartyi*
638 195. Expression of these enzymes was apparent by SDS-PAGE; however, no activity was ever
639 detected from the expression culture lysates. The details of all conditions tested for the expression
640 of these RDases can be found in the Supplemental Information Text 4.

641 The inability to achieve activity from the *Dehalococcoides* spp. enzymes could be due to
642 the absence of an unknown component required for folding such as an organism-specific
643 chaperone protein. Further work is needed to test more expression conditions for RDases from the
644 Chloroflexi *Dehalococcoides* and *Dehalogenimonas* to identify the essential factors in their
645 production. Nevertheless, the system we have presented provides an excellent starting point for
646 future efforts.

647 **Significance and future work**

648 Developing a heterologous system for RDase expression in *E. coli* has been a goal of the
649 dehalogenation community for the past several decades. Here we have presented a solution for the
650 expression of *Dehalobacter* derived RDases that will allow high yield expression and purification,
651 enabling future structural and mechanistic studies. We demonstrated that this system was able to
652 be applied to various RDases from *Dehalobacter* having as little as 28% amino acid sequence
653 identity to each other. Given the high similarity between *Dehalobacter* and *Desulfitobacterium*
654 RDases, we predict that this system would perform similarly for RDases from other Firmicutes.

655 We anticipate that this expression system will expedite the characterization of the RDase
656 enzyme family and advance the future of enzyme-driven bioremediation. Mutational studies can
657 now be carried out to identify key amino acids required for activity and specificity. The impact of
658 the type of corrinoid incorporated into the RDase on activity and substrate range can also be more
659 definitively investigated. However, the current standard assays used in this work require
660 development of analytical methods and individual standards for each substrate and product to
661 detect activity; a general assay to measure non-specific activity would allow data to be obtained
662 more quickly and would facilitate high-throughput analysis.

663 This work also has many implications for bioremediation. Individual RDases can be
664 screened on wider substrates panels to better delineate substrate ranges and to quantify effects of
665 putative inhibitors. This knowledge would better inform the choice of bioaugmentation culture(s)
666 when targeting complex contamination sites. Furthermore, this expression system will also allow
667 the functional determination for the huge number of undescribed *rdhA* genes present in
668 metagenomes, which in turn could identify novel candidate organisms for bioremediation. Finally,
669 having an established expression method in *E. coli* gives the opportunity to rationally engineer and
670 evolve RDases to dehalogenate emerging and highly halogenated compounds. However, two
671 bottlenecks that still must be addressed to truly jumpstart the future studies of RDases are 1)
672 generalizing or extending the assay to Chloroflexi, and 2) developing a high-throughput and
673 generalizable assay to make data production quicker and allow for the testing of a wide array of
674 substrates and enzymes.

675 In conclusion, we demonstrate the necessity of cobalamin and anaerobic conditions for the
676 heterologous expression of respiratory RDases from obligate OHRB. The implementation of the
677 *pBAD42-BtuCEDFB* expression vector allowed for the active expression of RDases in *E. coli*,
678 making this the first report of respiratory RDases actively expressed from *E. coli*. We demonstrated
679 that this system is easy to modify and was widely applicable within the *Dehalobacter* genus by
680 expressing and obtaining activity from six unique RDases. The expressed RDases were able to be
681 purified at high yields making this system useful for future analyses that require a lot of material.
682 We expect that this expression system will allow for the study and characterization of many
683 RDases that have so far remained elusive.

684

685

686 **ACKNOWLEDGEMENTS**

687 This study was supported by the National Sciences and Engineering Research Council of
688 Canada (NSERC PGS-D to KJP) and a Canadian Research Chair to EAE.

689 EAE and KJP conceived of the experiments. RF performed the LC-MS separation and
690 analysis of cobalamin, and KJP conducted all other experiments. KJP and EAE drafted the
691 manuscript.

692 We would like to thank the Booker Lab from Pennsylvania State University for gifting the
693 *pBAD42-BtuCEDFB* plasmid, and the Antony Lab from the St. Louis University School of
694 Medicine and Kiley lab from the University of Wisconsin-Madison for gifting us the *E. coli*
695 SufFeScient and *ara-Suf ΔiscR* strains. We would like to thank Connor Bowers for cloning and
696 testing the activity of the SUMO fusion constructs. We would like to thank Anna Khusnutdinova
697 for helpful advice in working with anaerobic enzymes and more generally the Yakunin and
698 Savchenko labs at the University of Toronto for sharing expression vectors and several RDase
699 constructs, and for their support during this study. Finally, we would like to thank Prof. Patrick
700 Hellenbeck for providing the *E. coli ΔiscR* strain.

701

702 **REFERENCES**

703 1. Mohn WW, Tiedje JM. 1990. Strain DCB-1 conserves energy for growth from reductive
704 dechlorination coupled to formate oxidation. *Arch Microbiol Microbiol* 153:267–271.

705 2. Hug LA, Maphosa F, Leys D, Löffler FE, Smidt H, Edwards EA, Adrian L. 2013.
706 Overview of organohalide-respiring bacteria and a proposal for a classification system for
707 reductive dehalogenases. *Philos Trans R Soc B* 368:20120322.

708 3. Duhamel M, Edwards EA. 2006. Microbial composition of chlorinated ethene-degrading
709 cultures dominated by *Dehalococcoides*. *FEMS Microbiol Ecol* 58:538–549.

710 4. Grostern A, Edwards EA. 2006. Growth of *Dehalobacter* and *Dehalococcoides* spp.
711 during degradation of chlorinated ethanes. *Appl Environ Microbiol* 72:428–436.

712 5. Ni S, Fredrickson JK, Xun L. 1995. Purification and characterization of a novel 3-
713 chlorobenzoate-reductive dehalogenase from the cytoplasmic membrane of *Desulfomonile*
714 *tiedjei* DCB-1. *J Bacteriol* 177:5135–5139.

715 6. Fincker M, Spormann AM. 2017. Biochemistry of catabolic reductive dehalogenation.
716 *Annu Rev Biochem* 86:357–386.

717 7. Chen K, Huang L, Xu C, Liu X, He J, Zinder SH, Li S, Jiang J. 2013. Molecular
718 characterization of the enzymes involved in the degradation of a brominated aromatic
719 herbicide. *Mol Microbiol* 89:1121–1139.

720 8. Payne KAP, Quezada CP, Fisher K, Dunstan MS, Collins FA, Sjuts H, Levy C, Hay S,
721 Rigby SEJ, Leys D. 2015. Reductive dehalogenase structure suggests a mechanism for
722 B₁₂-dependent dehalogenation. *Nature* 517:513–516.

723 9. Molenda O, Puentes Jácome LA, Cao X, Nesbø CL, Tang S, Morson N, Patron J,
724 Lomheim L, Wishart DS, Edwards EA. 2020. Insights into origins and function of the
725 unexplored majority of the reductive dehalogenase gene family as a result of genome
726 assembly and ortholog group classification. *Environ Sci Process Impacts* 22:663–678.

727 10. Futagami T, Morono Y, Terada T, Kaksonen AH, Inagaki F. 2009. Dehalogenation
728 activities and distribution of reductive dehalogenase homologous genes in marine
729 subsurface sediments. *Appl Environ Microbiol* 75:6905–6909.

730 11. Hug LA, Edwards EA. 2013. Diversity of reductive dehalogenase genes from
731 environmental samples and enrichment cultures identified with degenerate primer PCR
732 screens. *Front Microbiol* 4:341.

733 12. Magnuson JK, Stern R V., Gossett JM, Zinder SH, Burris DR. 1998. Reductive
734 dechlorination of tetrachloroethene to ethene by a two-component enzyme pathway. *Appl*
735 *Environ Microbiol* 64:1270–1275.

736 13. van de Pas BA, Gerritse J, de Vos WM, Schraa G, Stams AJM. 2001. Two distinct
737 enzyme systems are responsible for tetrachloroethene and chlorophenol reductive
738 dehalogenation in *Desulfitobacterium* strain PCE1. *Arch Microbiol* 176:165–169.

739 14. Jugder BE, Bohl S, Lebhar H, Healey RD, Manefield M, Marquis CP, Lee M. 2017. A
740 bacterial chloroform reductive dehalogenase: purification and biochemical
741 characterization. *Microb Biotechnol* 10:1640–1648.

742 15. Müller JA, Rosner BM, Von Abendroth G, Meshulam-Simon G, McCarty PL, Spormann
743 AM. 2004. Molecular identification of the catabolic vinyl chloride reductase from
744 *Dehalococcoides* sp. strain VS and its environmental distribution. *Appl Environ Microbiol*

745 70:4880–4888.

746 16. Bisailon A, Beaudet R, Lépine F, Déziel E, Villemur R. 2010. Identification and
747 characterization of a novel CprA reductive dehalogenase specific to highly chlorinated
748 phenols from *Desulfitobacterium hafniense* strain PCP-1. *Appl Environ Microbiol*
749 76:7536–7540.

750 17. Maillard J, Schumacher W, Vazquez F, Regeard C, Hagen WR, Holliger C. 2003.
751 Characterization of the corrinoid iron-sulfur protein tetrachloroethene reductive
752 dehalogenase of *Dehalobacter restrictus*. *Appl Environ Microbiol* 69:4628–4638.

753 18. Ye L, Schilhabel A, Bartram S, Boland W, Diekert G. 2010. Reductive dehalogenation of
754 brominated ethenes by *Sulfurospirillum multivorans* and *Desulfitobacterium hafniense*
755 PCE-S. *Environ Microbiol* 12:501–509.

756 19. Boyer A, Pagé-Bélanger R, Saucier M, Villemur R, Lépine F, Juteau P, Beaudet R. 2003.
757 Purification, cloning and sequencing of an enzyme mediating the reductive dechlorination
758 of 2,4,6-trichlorophenol from *Desulfitobacterium frappieri* PCP-1. *Biochem J* 373:297–
759 303.

760 20. Krasotkina J, Walters T, Maruya KA, Ragsdale SW. 2001. Characterization of the B₁₂-
761 and iron-sulfur-containing reductive dehalogenase from *Desulfitobacterium*
762 *chlororespirans*. *J Biol Chem* 276:40991–40997.

763 21. van de Pas BA, Smidt H, Hagen WR, van der Oost J, Schraa G, Stams AJM, de Vos WM.
764 1999. Purification and molecular characterization of *ortho*-chlorophenol reductive
765 dehalogenase, a key enzyme of halorespiration in *Desulfitobacterium dehalogenans*. *J*
766 *Biol Chem* 274:20287–20292.

767 22. Christiansen N, Ahring BK, Wohlfarth G, Diekert G. 1998. Purification and
768 characterization of the 3-chloro-4-hydroxy-phenylacetate reductive dehalogenase of
769 *Desulfitobacterium hafniense*. FEBS Lett 436:159–162.

770 23. Thibodeau J, Gauthier A, Duguay M, Villemur R, Lépine F, Juteau P, Beaudet R. 2004.
771 Purification, cloning, and sequencing of a 3,5-dichlorophenol reductive dehalogenase
772 from *Desulfitobacterium frappieri* PCP-1. Appl Environ Microbiol 70:4532–4537.

773 24. Tang S, Chan WWM, Fletcher KE, Seifert J, Liang X, Löffler FE, Edwards EA, Adrian L.
774 2013. Functional characterization of reductive dehalogenases by using blue native
775 polyacrylamide gel electrophoresis. Appl Environ Microbiol 79:974–981.

776 25. Liang X, Molenda O, Tang S, Edwards EA. 2015. Identity and substrate specificity of
777 reductive dehalogenases expressed in *Dehalococcoides*-containing enrichment cultures
778 maintained on different chlorinated ethenes. Appl Environ Microbiol 81:4626–4633.

779 26. Adrian L, Rahnenführer J, Gobom J, Hölscher T. 2007. Identification of a chlorobenzene
780 reductive dehalogenase in *Dehalococcoides* sp. strain CBDB1. Appl Environ Microbiol
781 73:7717–7724.

782 27. Tang S, Edwards EA. 2013. Identification of *Dehalobacter* reductive dehalogenases that
783 catalyse dechlorination of chloroform, 1,1,1- trichloroethane and 1,1-dichloroethane.
784 Philos Trans R Soc B Biol Sci 368.

785 28. Molenda O, Quaile AT, Edwards EA. 2016. *Dehalogenimonas* sp. strain WBC-2 genome
786 and identification of its *trans*-dichloroethene reductive dehalogenase, TdrA. Appl Environ
787 Microbiol 82:40–50.

788 29. Alfán-Guzmán R, Ertan H, Manefield M, Lee M. 2017. Isolation and characterization of
789 *Dehalobacter* sp. strain TeCB1 including identification of TcbA: A novel tetra- and
790 trichlorobenzene reductive dehalogenase. *Front Microbiol* 8:558.

791 30. Neumann A, Wohlfarth G, Diekert G. 1998. Tetrachloroethene dehalogenase from
792 *Dehalospirillum multivorans*: Cloning, sequencing of the encoding genes, and expression
793 of the pceA gene in *Escherichia coli*. *J Bacteriol* 180:4140–4145.

794 31. Suyama A, Yamashita M, Yoshino S, Furukawa K. 2002. Molecular characterization of
795 the PceA reductive dehalogenase of *Desulfitobacterium* sp. strain Y51. *J Bacteriol*
796 184:3419–3425.

797 32. Sjuts H, Fisher K, Dunstan MS, Rigby SE, Leys D. 2012. Heterologous expression,
798 purification and cofactor reconstitution of the reductive dehalogenase PceA from
799 *Dehalobacter restrictus*. *Protein Expr Purif* 85:224–229.

800 33. Mac Nelly A, Kai M, Svatoš A, Diekert G, Schubert T. 2014. Functional heterologous
801 production of reductive dehalogenases from *Desulfitobacterium hafniense* strains. *Appl
802 Environ Microbiol* 80:4313–4322.

803 34. Bommer M, Kunze C, Fesseler J, Schubert T, Diekert G, Dobbek H. 2014. Structural basis
804 for organohalide respiration. *Science* (80-) 346:455–458.

805 35. Jugder B-E, Payne KAP, Fisher K, Bohl S, Lebhar H, Manefield M, Lee M, Leys D,
806 Marquis CP. 2018. Heterologous production and purification of a functional chloroform
807 reductive dehalogenase. *ACS Chem Biol* 13:548–552.

808 36. Kunze C, Diekert G, Schubert T. 2017. Subtle changes in the active site architecture

untangled overlapping substrate ranges and mechanistic differences of two reductive dehalogenases. *FEBS J* 284:3520–3535.

37. Parthasarathy A, Stich TA, Lohner ST, Lesnfsky A, Britt RD, Spormann AM. 2015. Biochemical and EPR-spectroscopic investigation into heterologously expressed vinyl chloride reductive dehalogenase (VcrA) from *Dehalococcoides mccartyi* strain VS. *J Am Chem Soc* 137:3525–3532.

38. Nakamura R, Obata T, Nojima R, Hashimoto Y, Noguchi K, Ogawa T, Yohda M. 2018. Functional expression and characterization of tetrachloroethene dehalogenase from *Geobacter* sp. *Front Microbiol* 9:1774.

39. Fang H, Kang J, Zhang D. 2017. Microbial production of vitamin B₁₂: a review and future perspectives. *Microb Cell Fact* 16:15.

40. Bassford PJ, Kadner RJ. 1977. Genetic analysis of components involved in vitamin B₁₂ uptake in *Escherichia coli*. *J Bacteriol* 132:796–805.

41. Cadieux N, Bradbeer C, Reeger-Schneider E, Köster W, Mohanty AK, Wiener MC, Kadner RJ. 2002. Identification of the periplasmic cobalamin-binding protein BtuF of *Escherichia coli*. *J Bacteriol* 184:706–717.

42. Borths EL, Poolman B, Hvorup RN, Locher KP, Rees DC. 2005. In vitro functional characterization of BtuCD-F, the *Escherichia coli* ABC transporter for vitamin B₁₂ uptake. *Biochemistry* 44:16301–16309.

43. Hvorup RN, Goetz BA, Niederer M, Hollenstein K, Perozo E, Locher KP. 2007. Asymmetry in the structure of the ABC transporter-binding protein complex BtuCD-BtuF.

830 Science (80-) 317:1387–1390.

831 44. Lanz ND, Blaszczyk AJ, McCarthy EL, Wang B, Wang RX, Jones BS, Booker SJ. 2018.

832 Enhanced solubilization of class B radical S-adenosylmethionine methylases by improved

833 cobalamin uptake in *Escherichia coli*. Biochemistry 57:1475–1490.

834 45. DeVeaux LC, Kadner RJ. 1985. Transport of vitamin B₁₂ in *Escherichia coli*: Cloning of

835 the *btuCD* region. J Bacteriol 162:888–896.

836 46. Shultis DD, Purdy MD, Banchs CN, Wiener MC. 2006. Outer membrane active transport:

837 Structure of the BtuB:TonB complex. Science 312:1396–1399.

838 47. Blaszczyk AJ, Wang RX, Booker SJ. 2017. TsrM as a model for purifying and

839 characterizing cobalamin-dependent radical S-adenosylmethionine methylases. Methods

840 Enzymol 595:303–329.

841 48. Halliwell T, Fisher K, Payne K, Rigby SEJ, Leys D. 2021. Heterologous expression of

842 cobalamin dependent class-III enzymes. Protein Expr Purif 177:105743.

843 49. Akhtar MK, Jones PR. 2008. Deletion of *iscR* stimulates recombinant clostridial Fe-Fe

844 hydrogenase activity and H₂-accumulation in *Escherichia coli* BL21(DE3). Appl

845 Microbiol Biotechnol 78:853–862.

846 50. Kuchenreuther JM, Grady-Smith CS, Bingham AS, George SJ, Cramer SP, Swartz JR.

847 2010. High-yield expression of heterologous [FeFe] hydrogenases in *Escherichia coli*.

848 PLoS One 5:e15491.

849 51. Corless EI, Mettert EL, Kiley PJ, Antony E. 2020. Elevated expression of a functional Suf

850 pathway in *Escherichia coli* BL21(DE3) enhances recombinant production of an iron-

851 sulfur cluster-containing protein. *J Bacteriol* 202:e00496-19.

852 52. Almagro Armenteros JJ, Tsirigos KD, Sønderby CK, Nordahl Petersen T, Winther O,
853 Brunak S, von Heijne G, Nielsen H. 2019. SignalP 5.0 improves signal peptide predictions
854 using deep neural networks. *Nat Biotechnol* 37:420–423.

855 53. Jaganaman S, Pinto A, Tarasev M, Ballou DP. 2007. High levels of expression of the
856 iron–sulfur proteins phthalate dioxygenase and phthalate dioxygenase reductase in
857 *Escherichia coli*. *Protein Expr Purif* 52:273–279.

858 54. Riemer J, Hoepken HH, Czerwinska H, Robinson SR, Dringen R. 2004. Colorimetric
859 ferrozine-based assay for the quantitation of iron in cultured cells. *Anal Biochem*
860 331:370–375.

861 55. Fish WW. 1988. Rapid colorimetric micromethod for the quantification of complexed iron
862 in biological samples. *Methods Enzymol* 158:357–364.

863 56. Yan J, Im J, Yang Y, Löffler FE. 2013. Guided cobalamin biosynthesis supports
864 *Dehalococcoides mccartyi* reductive dechlorination activity. *Philos Trans R Soc B*
865 368:20120320.

866 57. Yan J, Bi M, Bourdon AK, Farmer AT, Wang P-H, Molenda O, Quaile AT, Jiang N, Yang
867 Y, Yin Y, Burcu Ş, Campagna SR, Edwards EA, Löffler FE. 2018. Purinyl-cobamide is a
868 native prosthetic group of reductive dehalogenases. *Nat Chem Biol* 14:8–14.

869 58. Wang P-H. 2018. Essential cofactors in anaerobic microbial consortia used for
870 bioremediation: Biosynthesis, function, and regeneration. University of Toronto.

871 59. Chan WWM. 2010. Characterization of Reductive Dehalogenases in a Chlorinated

872 Ethene-Degrading Bioaugmentation Culture. University of Toronto.

873 60. Wang P-H, Tang S, Nemr K, Flick R, Yan J, Mahadevan R, Yakunin AF, Löffler FE,
874 Edwards EA. 2017. Refined experimental annotation reveals conserved corrinoid
875 autotrophy in chloroform-respiring *Dehalobacter* isolates. ISME J 11:626–640.

876 61. Grostern A, Edwards EA. 2006. A 1,1,1-trichloroethane-degrading anaerobic mixed
877 microbial culture enhances biotransformation of mixtures of chlorinated ethenes and
878 ethanes. Appl Environ Microbiol 72:7849–7856.

879 62. Puentes Jácome LA. 2019. Anaerobic biodegradation of chlorinated benzenes and
880 hexachlorocyclohexane by mixed microbial cultures derived from contaminated field
881 sites. University of Toronto.

882 63. Qiao W, Puentes Jácome LA, Tang X, Lomheim L, Yang MI, Gaspard S, Avanzi IR, Wu
883 J, Ye S, Edwards EA. 2020. Microbial communities associated with sustained anaerobic
884 reductive dechlorination of α -, β -, γ -, and δ -hexachlorocyclohexane isomers to
885 monochlorobenzene and benzene. Environ Sci Technol 54:255–265.

886 64. Rupakula A, Kruse T, Boeren S, Holliger C, Smidt H, Maillard J. 2013. The restricted
887 metabolism of the obligate organohalide respiring bacterium *Dehalobacter restrictus*:
888 lessons from tiered functional genomics. Philos Trans R Soc B 368:20120325.

889